5-2018

In Vitro Aortic Arch Flow Model For Vector Flow Imaging Testing

Jackson Mosley
University of Arkansas, Fayetteville

In Vitro Aortic Arch Flow Model for Vector Flow Imaging Testing

Honors Thesis Dissertation by Jackson Mosley

Department of Biomedical Engineering

College of Engineering

University of Arkansas

Honors Advisor: Dr. Hanna Jensen

Honors Coordinator: Dr. Kyle Quinn

Abstract

Pediatric stenosis is the narrowing of the aorta at the aortic valve, above the aortic valve, or below the aortic valve. Typically, this disease's severity is diagnosed by conventional Doppler ultrasound methods, or echocardiography. Conventional Doppler can sometimes overestimate the pressure gradient over the area of stenosis, diagnosing some cases of PAS to be more severe than they actually are. This causes earlier intervention than is desired in children. A new US modality, Vector Flow Imaging (VFI), is an angle-independent US imaging method that can potentially more accurately quantify peak blood flow velocities and pressure gradients across stenotic sections of vasculature. This project's goal was to create an in vitro cardiac flow loop that could validate the accuracy with which VFI could obtain these measurements. An in vitro healthy aortic arch was created so that pressure gradients could be measured directly by pressure transducers located at the inlet and outlet of the stenosis and compared to the pressure gradients obtained across the same region by use of VFI. A LabView VI was designed to display pressure vs. time data in Excel to obtain these pressure measurements. A mechanical pump was also designed to create pulsatile flow throughout the loop.

Introduction

Pediatric aortic stenosis (PAS) is the narrowing of the aorta in children, obstructing the flow of blood pumped from the left ventricle. This congenital heart defect can exist as valvar, subvalvar, or supravalvar AS [1]. AS is incident in 5% of children diagnosed with heart disease [1].

Valvar aortic stenosis, or VAS, is the most common obstruction to left ventricular flow [1]. In adults, VAS manifests as a sclerotic aortic valve with thickened leaflets that eventually

becomes inflamed or calcified. [2] A reduction in the area of the orifice will occur in the beginning of the onset of the stenosis when the valve is sclerotic and will continue to narrow until the valve becomes calcified. [2] Aortic valves normally exist as tricuspid tissue valves, valves with three leaflets or cusps. Being born with an abnormal bicuspid valve predisposes a person to a higher likelihood of developing aortic stenosis because of a differing functionality of the valve. [2]

If aortic stenosis is present in a young infant, it is called neonatal critical aortic stenosis, and is nearly always fatal if there is no surgical intervention [1]. This case of AS in children typically occurs when there is a bicuspid or sclerotic valve with a reduced cross- sectional area. [1] In both children and in adults, the reduction in cross-sectional area at the valve results in an elevated pressure gradient across the stenosis that puts significant strain on the left ventricle. [2] This can result in concomitant anomalies such as left ventricular hypertrophy, where the cardiac myocytes of the left ventricle enlarge to try and compensate for the elevated load requirement placed on the heart. [2]

Supravalvar aortic stenosis (SVAS) is the most common cardiovascular anomaly in William's Syndrome. [3] William's Syndrome is a "congenital, multisystem disorder involving the cardiovascular, connective tissue, and central nervous systems." [4] It is characterized and diagnosed on the basis of many phenotypic characteristics such as stellate eyes, a broad forehead, and full lips. [3] In this population of children, SVAS is manifested in one of two ways. It either exists as an hourglass-shaped narrowing of the aorta near the sinotubular junction or a diffuse stenosis of the ascending aorta. [3] Both instances result in a narrowing of a section of the aorta that introduce abnormal hemodynamics in that section. These complications in conjunction with common concomitant problems of SVAS such as coronary perfusion [5] make correctional

surgery a requirement for SVAS. SVAS correctional surgery is usually done by patch aortoplasty (using a synthetic patch to widen a section of the aorta) and sometimes by multi-sinus repair [1].

Subvalvar aortic stenosis (SAS) is one of the more rare forms of PAS, making up only 8 to 10% of all congenital aortic stenosis [6]. It is not always characterized by discrete symptoms or pathologies, but more-so by a spectrum. [1] The most common form is a "discrete ridge of fibrous tissue that projects into the left ventricle completely circling the outflow tract." [7] Some cases of this type of SAS include bulging and hypertrophy of the interventricular septum underneath. [7] Sometimes, if there is hypertrophy of just the septum and left ventricle, the thickened muscle will come together during left ventricular contraction and occlude the path to the systemic circulation. [7] Angina, dyspnea, and palpitations are some of the common symptoms of SAS. [7] Correctional operations for SAS are usually very low risk. [6]

All three levels of pediatric aortic stenosis share a few commonalities. First, every type's underlying problem is an obstruction to the systemic circulation. This obstruction or narrowing of a particular point in the aorta will substantially raise the pressure and maximum velocity of the blood flowing over that stenotic region. Second, symptomatic children have a poor prognosis and require intervention [2]. Third, and finally, careful consideration must be taken into each type of surgical intervention, because children are the recipient of such intervention. Whether the intervention be an aortic valve replacement or an aortoplasty, because it is being done in a child, it will almost certainly not be the last correctional procedure required to fix the disease. Children's bodies, both internally and externally, continue to grow. Because most replacement aortic valves or grafts will not continue to grow with the child, they will soon be too small to support healthy systemic circulation, and subsequent operations will have to be performed. Thus, to avoid continual and potentially risky operations, it is best to surgically intervene at the latest

possible moment. This means that diagnosing the severity of the stenosis is almost more important than diagnosing the stenosis itself. In children, the surgeon should only operate on the child when there is no other choice - when the stenosis is most severe.

Transthoracic echocardiography or Doppler echocardiography is the standard imaging modality for diagnosing PAS and determining its severity. [2] This ultrasound modality works by measuring the jet velocity of blood across the stenosis. [2] Multiple views or angles are required to correctly identify the maximum stenotic jet velocity. [2] Common transducer angles that yield the highest velocity are the apical, suprasternal, and right parasternal views [2]. After the peak velocity across the stenosis is correctly identified, the simplified Bernoulli equation can be used to obtain the mean and maximum pressure gradients across the area of stenosis. [2] These are termed, ΔP_{mean} and , ΔP_{max}, respectively. [2] The simplified Bernoulli equation is given below.

$$\Delta P = 4V^2$$

Equation 1: The simplified Bernoulli equation. ΔP represents the pressure gradient, while V is the peak blood flow velocity measured by ultrasound. [8]

The most direct way of measuring the pressure gradient across the area of stenosis is by using cardiac catheterization. This method is not ideal for pediatric patients because of its invasiveness and cost compared to using a bed-side imaging modality such as Doppler echocardiography. Unfortunately, there exists a discrepancy between the pressure measurements taken across the aorta from echocardiography versus cardiac catheterization. [2] When the blood flows across the stenosis into the ascending aorta, a portion of the blood's kinetic energy is converted back into potential energy. [2] This increases the local pressure, and is known as the pressure recovery effect. [2] The direct pressure gradient taken across the stenosis by

catheterization is termed, ΔP_{rec}, owing to pressure recovery. [2] Doppler echocardiography does not take this pressure recovery effect into consideration when obtaining the pressure gradient across the aortic stenosis. [2] It only measures the maximum jet velocity from different angles, which can be used to find ΔP_{max}. [2] Because this does not take into account the loss of kinetic energy by the pressure recovery effect, Doppler can overestimate the local velocity, in turn overestimating the stenotic pressure gradient. [2] Thus, the elevated pressure gradients obtained from Doppler echocardiography can lead physicians to believe that a case of pediatric aortic stenosis may be more severe than it actually is, and will refer the patient to a high-risk surgery that may not be fully necessary at that time. A new imaging modality that can obtain these pressure gradients more reliably and accurately is needed in pediatric cardiology.

Physicians believe they may have found the answer in a new more comprehensive form of blood flow imaging known as Vector Flow Imaging (VFI). Vector flow imaging is essentially a vector flow ultrasound system that can provide "real-time, angle-independent estimates of cardiac blood flow." [9] As opposed to Doppler ultrasound, which can only take velocity measurements in one dimension, VFI is capable of providing the user with two dimensional velocity components. Doppler ultrasound is angle-dependent because it can only obtain and provide the axial component of blood velocity, or the component of the velocity in the same direction as the ultrasound beam. [10] So, it does not give the full magnitude of the blood velocity vector, but only the "vector velocity projected onto the axis of the ultrasound beam direction." [10] VFI, however, can obtain and measure the axial and transverse components of the flow velocity. [11] This allows for more accurate characterization of complex blood flow that is often obscured by the one dimensional, angle dependent velocity estimation of Doppler

ultrasound. [12,13] It also gives blood velocity vector magnitudes that are more accurate and representative of the actual blood flow occurring in the vessel of interest.

Transverse oscillation is the underlying mechanism of VFI that gives this novel ultrasound technology the ability to obtain the transverse and axial velocity components of blood flow. Conventional ultrasound works by emitting an oscillatory echo field in the axial direction at a certain frequency. [10] Blood scatterers will emit back a frequency that is measured by the transducer along the axial direction, f_z. [10] This, then, only gives a velocity component of the blood in the same direction as the emitted and detected frequency. [10] This velocity component is v_z. [10] Transverse oscillation obtains an axial, v_z, and transverse velocity component, v_x, by emitting two oscillating pulse echo fields in the transverse and axial directions. [10] To make a transverse oscillatory echo component, the apodization of the receive aperture is adjusted so that the whole aperture has two point sources. [10] These two point sources create an oscillatory field with grating lobes that give rise to the transverse oscillation. [10]. Blood scatterers in these two fields will emit frequencies measured by the transducer in both the x and z directions, f_x and f_z, respectively. [10] These two frequencies are proportional to their respective blood velocity vectors that can be used to find the magnitude of the overall blood velocity vector. [10] An illustration of the measured velocity components and the relationship between the measured frequencies and velocity components are shown below.

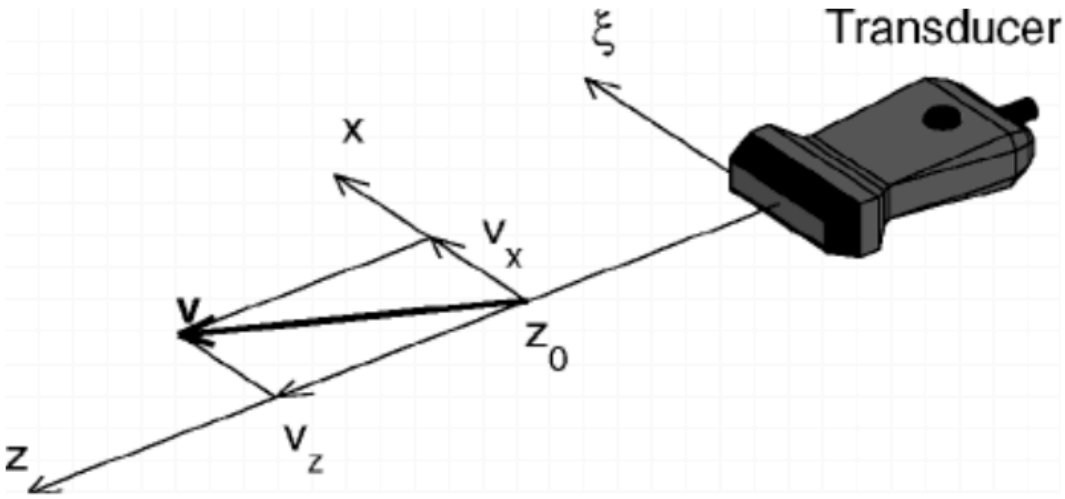

Figure 1: A diagram showing how a TO transducer can obtain blood velocity vectors in two dimensions to obtain an overall magnitude of the blood velocity vector, **v**. [10]

The overall magnitude of the blood velocity vectors at multiple points can therefore be more accurately measured by resolving each vector into two dimensional components. This better characterizes blood flow than conventional ultrasound methods in multiple ways. First, it can better characterize non-conventional or non-laminar flow patterns that often occur in diseased vessels or over areas of stenosis. [14] For example, the direction of different blood flow velocity vectors proved in a study that increased helical and more complex blood flow is sometimes characteristic of flow through stenotic aortic valves. [14] Figure 2 shows data taken from patients in that study that compare blood flow over normal aortic valves to that of stenotic aortic valves. [14] The two-dimensional velocity vectors captured with VFI illustrate the complex nature of blood flow over areas of stenosis and give a more detailed characterization of the flow than conventional Doppler would, primarily because of its angle-dependent limitation. [14] VFI, in theory, should also be better than conventional ultrasound for diagnosing the severity of aortic stenosis. VFI vectors give a more accurate magnitude of peak velocities than conventional ultrasound because they are resolved into two components. Recall that to quantify pressure gradients from ultrasound, the peak blood flow velocity is used in the simplified Bernoulli equation. [2] Because VFI can quantify velocity more accurately, even estimations of pressure from equations like the simplified Bernoulli will be more accurate than estimations of pressure from conventional ultrasound imaging methods.

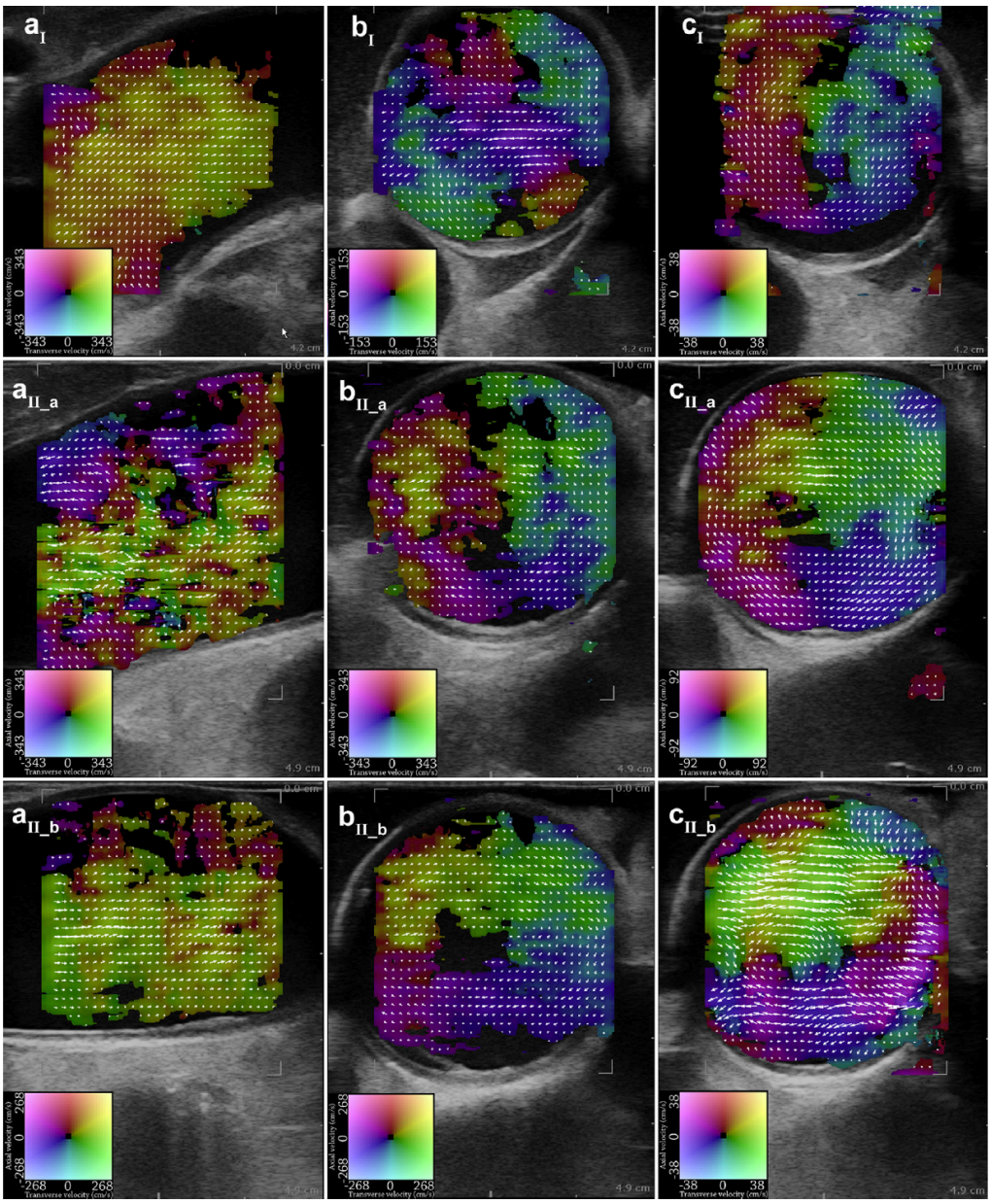

Fig. 2. Scans of one patient with a normal aortic valve (group I) and one patient with aortic valve stenosis before (group IIa) and after (group IIb) valve replacement. (a) Recordings in long-axis view during systole. (b,c) Recordings in short-axis view during systole (b) and diastole (c). The flow angle of the vector velocity correlates to the pixel color, whereas the flow magnitude correlates to pixel intensity as indicated by the color map and the superimposed vector arrows. Patient group is denoted by the subscript.

Figure 2: Multiple images of the aortic valve taken by VFI that illustrate its ability to characterize unique patterns of blood flow by giving two dimensional blood velocity vectors. Each picture's context is given in the original author's description. [14]

Physicians are hoping that more accurate pressure readings from a bedside, noninvasive imaging method such as VFI ultrasound will give a more realistic representation of the severity of pediatric aortic stenosis in children. This way, more unnecessary open surgeries for moderate to low risk aortic stenosis in children will be avoided.

More hospitals and clinicians are becoming interested in this new technology for their own pediatric patients. This study wanted to provide an in vitro method for validating the accuracy with which VFI can obtain pressure measurements. More specifically, we wanted to verify the accuracy with which the VFI can obtain a pressure gradient across a stenotic aortic arch. Our goal was to devise a cardiac flow loop in vitro that could verify the accuracy of VFI.

Materials and Methods

Flow Loop Components and Parameters

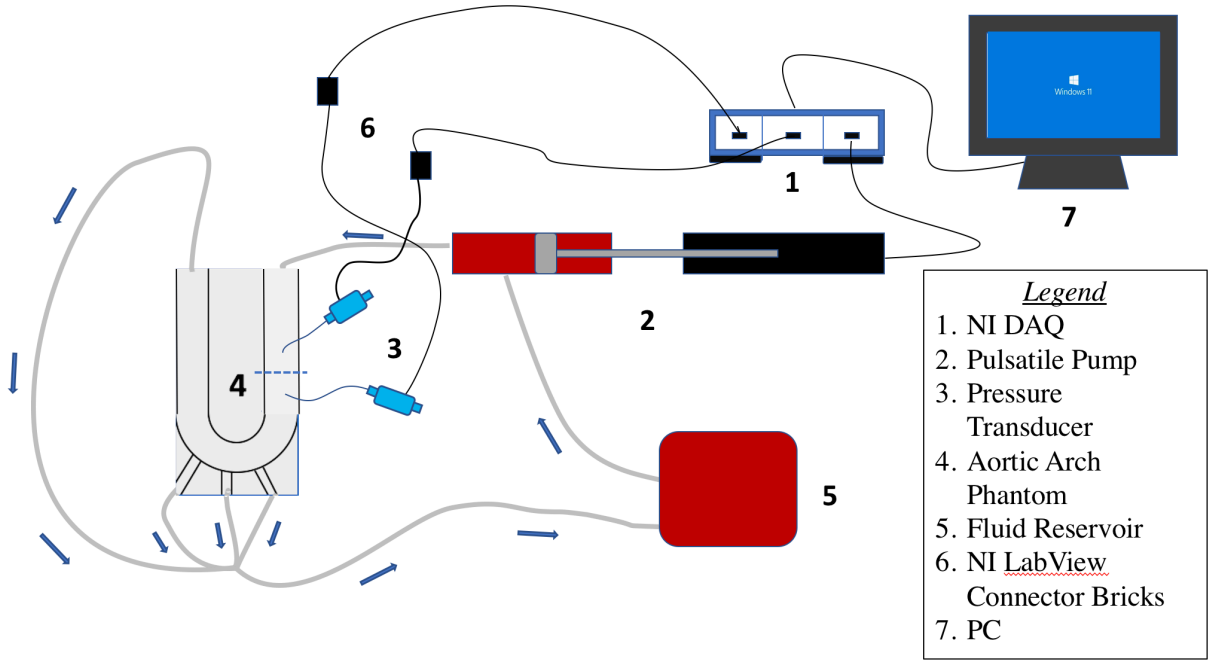

Figure 3: Diagram of in vitro cardiac flow loop inspired by Pasta et. al. [15]

Figure 3 illustrates the final design for the in vitro cardiac flow loop. This setup was inspired by the in vitro cardiac flow loop used in the Pasta et. al study. [15] Within the flow loop, multiple key components were present that needed to be functioning properly and operating within our physiological hemodynamic parameters listed in Table 1. A pulsatile pump capable of producing the specified cardiac output, heart rate, and systolic peak pressure was needed. Also needed were two pressure transducers with the peak systolic pressure parameter within its range of pressure readings. The other two key components were the aortic arch phantom and the NI DAQ. The aortic arch phantom would be a section of the aortic arch created in vitro that would be imaged with VFI while blood analog would be flowing through it in a pulsatile manner. Pressure gradients would be taken in this created vasculature to compare to the pressure gradients obtained in VFI. The NI DAQ would be the data acquisition device used to convert the analog signals taken by the pressure transducers into meaningful, time-varying pressure data in LabView 2014 software.

Table 1: Maximum hemodynamic parameters for the proposed in vitro cardiac flow loop.

Parameter	**Value**
Cardiac Output	6 L/min
Heart Rate	160 bpm (beats per minute)
Systolic Peak Pressure	250 mmHg

Pulsatile Pump

For the flow loop, pulsatile blood flow similar to that created by the heart was desired. Particular pressure waveforms are characteristic of this pulsatile flow in humans that was desired to be replicated by a mechanical pump. Pressure gradients through a stenotic aortic arch were of particular interest, and these pressure gradients are, for simplicity's sake, measured during peak systole in the diagnosis of aortic stenosis by direct methods. [2] Pulsatile flow comparable to that of the heart would produce a flow pattern with pressure peaks representative of this point in the cardiac cycle. Figure 4 is an image of the general pulsatile flow pattern of blood created by the heart and its division into various stages, including systole, that the mechanical pump would replicate.

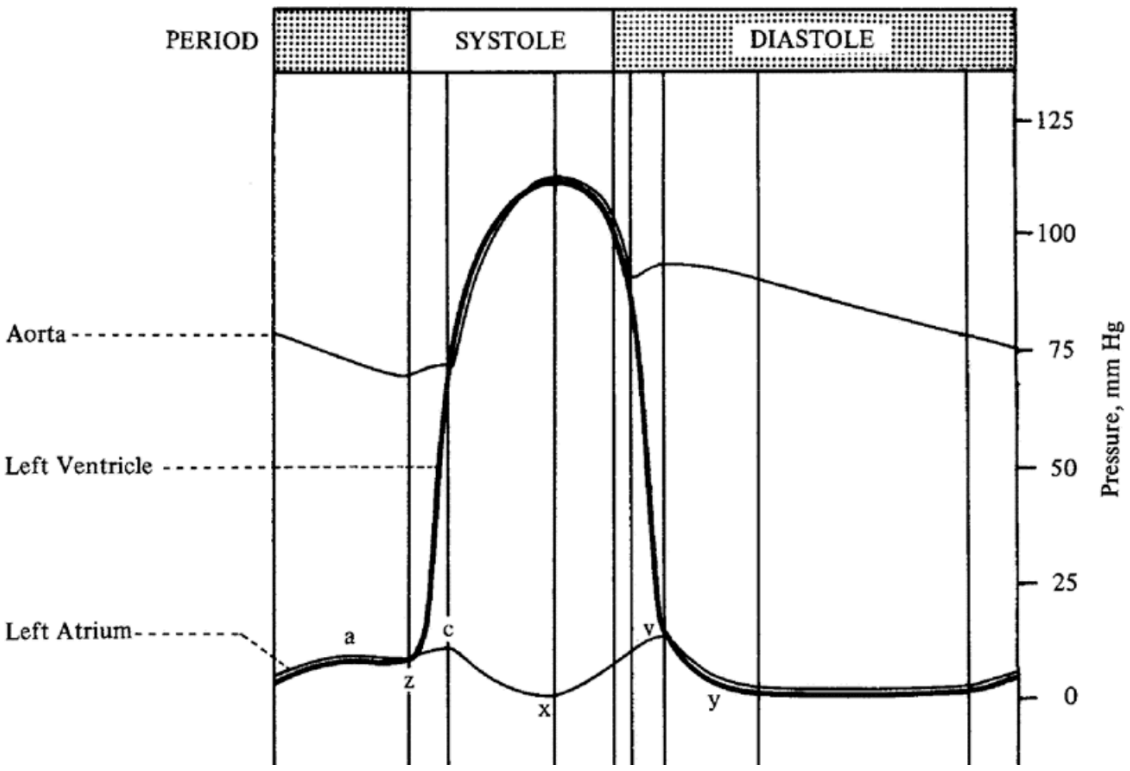

Figure 4: Diagram illustrating blood pressure change (in mmHg) during the cardiac cycle. [16]

This pump would operate as a piston pushing fluid out at a flow rate similar to that of the average cardiac output for a child in the age range specified. The stroke volume of our pump could be calculated by finding the volume of the container in the pump containing the blood analog and converting this measurement into liters. The heart rate of the pump would be user-controlled and pre-defined in the input to our pump. Ideally, the heart rate would be controlled. A pump having constant stroke volume with a variable heart rate would be a pump capable of producing a range of cardiac outputs, from normal to maximum hemodynamics parameters.

Aortic Arch Phantom

To properly replicate physiological conditions of pulsatile blood flow through an aortic arch in vitro, an in vitro artic arch needed to be created. Sections of vasculature created in vitro are typically referred to as phantoms.

Initially, the creation of an aortic arch phantom was desired to be identical to that of a pediatric patient for optimal physiological similarity. For this process, two MRI scans from pediatric aortic stenosis patients were saved onto CDs in the form of multiple DICOM images. DICOM images are essentially individual slices of an MRI that will form the entire scan if ordered correctly in software such as ImageJ. This process was designed to upload the series of DICOM images into ImageJ using the DICOM viewer plugin, have them re-ordered, isolate the aortic arch from the rest of the scan using ImageJ's polygon function, and then export the isolated vasculature into Blender software. Once in Blender software, it would be edited (effectively simplifying the shape of the vasculature to be more easily 3D printed) and exported as a .stl file to SOLIDWORKS software. This .stl file would then be read by an available 3D

printer, and printed. This 3D printed vasculature would be used by other methods to create a final patient-specific aortic phantom. An image of an example of a successfully created patient-specific aortic arch phantom is shown in Figure 5.

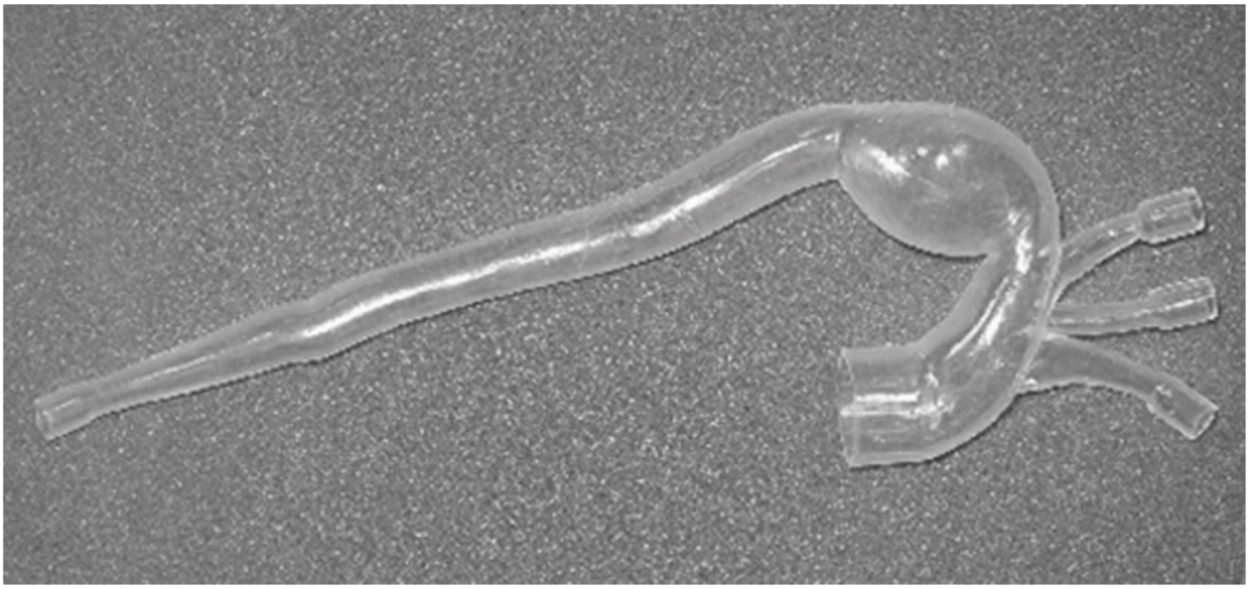

Figure 5: An aortic arch phantom with an aneurysm derived from patient MRI [17]

A patient-specific stenotic aortic arch phantom was unable to be created due to software complications and time constraints. A plan was designed to then create a healthy aortic arch phantom that could be used in the flow loop to test our validation techniques. Instead of having a lone in vitro vessel as our phantom, a block of cured molten material with an inner cavity in the shape of the aortic arch lumen was created.

To do this, a healthy aortic arch was drawn in SOLIDWORKS software. The diameter of the aorta and of the branching arteries were based on average healthy dimensions of these vessels derived from medical literature. An image of the final drawn healthy aortic arch is shown in Figure 6.

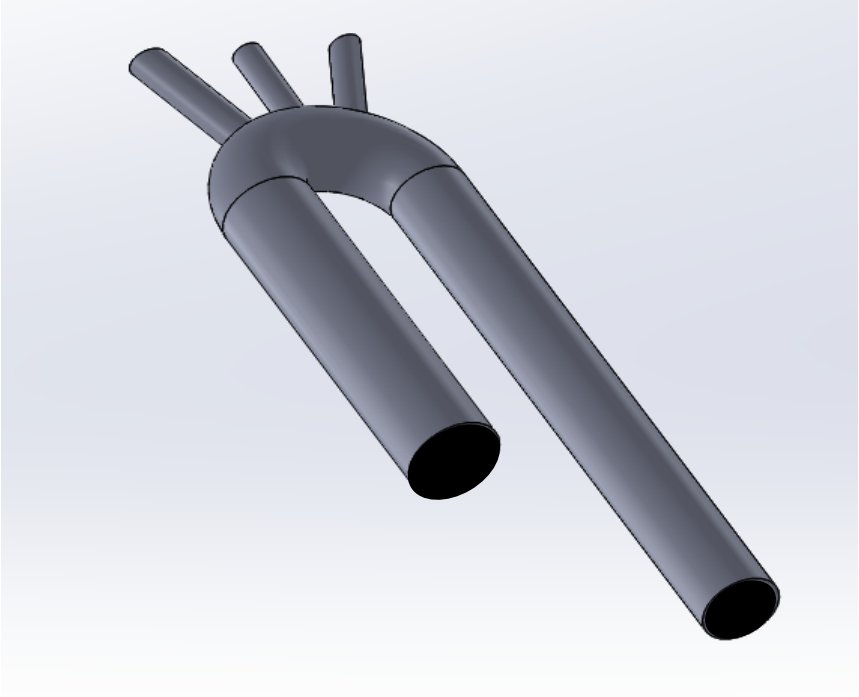

Figure 6: Healthy aortic arch drawn in SOLIDWORKS software

A box or container was then designed to contain the molten silicone. Included in the box design were holes corresponding to the diameters of the ascending and descending aortas as well as the three branches. The result would be the aortic arch suspended within the arch so that it lay in the middle of the silicone block when it cured. The box was designed to be composed of several different pieces that would snap together when assembled. All pieces were drawn in SOLIDWORKS software in separate .SLDPRT files and laser-cut out of acrylic material.

The silicone liquid mixture was poured and allowed to cure in the assembled acrylic box. The silicone was then allowed to completely cure. The acrylic box pieces were all removed.

Further design refinement and research into ballistics gel led to the consensus that it would be a better choice of material to create the aortic arch phantom. Its mechanical properties closely align with that of human tissue, making it an ideal choice for a material whose eventual purpose is to be imaged with VFI ultrasound technology. To get ultrasound images most

comparable to that of human tissue, it is best to image a material with an acoustic impedance close to that of human tissue, a property that ballistics gel has.

Studies conducted in the lab by other groups helped in the refinement of this design and the process of creating the desired phantom. It was found that ballistics gel does not react in the same way with metal material as it does with acrylic. As a result, a box to contain the molten gel was designed primarily out of metal. The metal base of the box was drawn in SOLIDWORKS software. This base was made of three sides, leaving the ends of the box open. The ends of the box were 3-D printed to allow easy removal of the box after curing of the ballistics gel.

Approximately at 500 cc of ballistics gel was prepared to be poured. A block of the gel was broken up into pieces and then put in a metal pitcher and melted at 275 degrees Fahrenheit. Once it was melted, it was vacuumed twice in the vacuum chamber for bubble removal. The gel was re-heated after each time it was vacuumed. The box was placed back in the refrigerator to keep the gel as cool as possible while it cured. Ideally, the gel is placed in the freezer, but there was not enough space for our setup.

Deltran II Pressure Transducers

The two pressure transducers in the proposed in vitro cardiac flow loop are the key components for validating the accuracy of VFI. To successfully validate this imaging technique, these transducers are used to measure the pressure gradient across the stenosis to compare to the pressure gradient obtained by the VFI. The pressure gradient would be measured by taking the peak systolic pressures at the inlet and outlet of the aortic stenosis and finding the difference between the two. Thus, the Deltran II pressure transducers needed to be capable of obtaining pressure vs. time measurements at the inlet and outlet of the area of stenosis in the aortic arch

phantom. National Instruments LabView 2014 software was used to convert the analog signals taken from the pressure transducers and converting them into digital signals to display meaningful pressure vs. time data. A block diagram in a VI was constructed for the extraction and display of this data. The pressure transducers were connected to NI 9949 terminal bricks that were then connected to a NI cDAQ-9174. A mini flow loop was set up to verify the functionality of the LabView code and to confirm that the pressure transducers obtained the data that was required. The data taken by the pressure transducers and displayed in LabView was written to an Excel file for display and analysis. Figures 7 and 8 show the set up of the mini flow loop and the block diagram used to extract pressure data form the transducers, respectively.

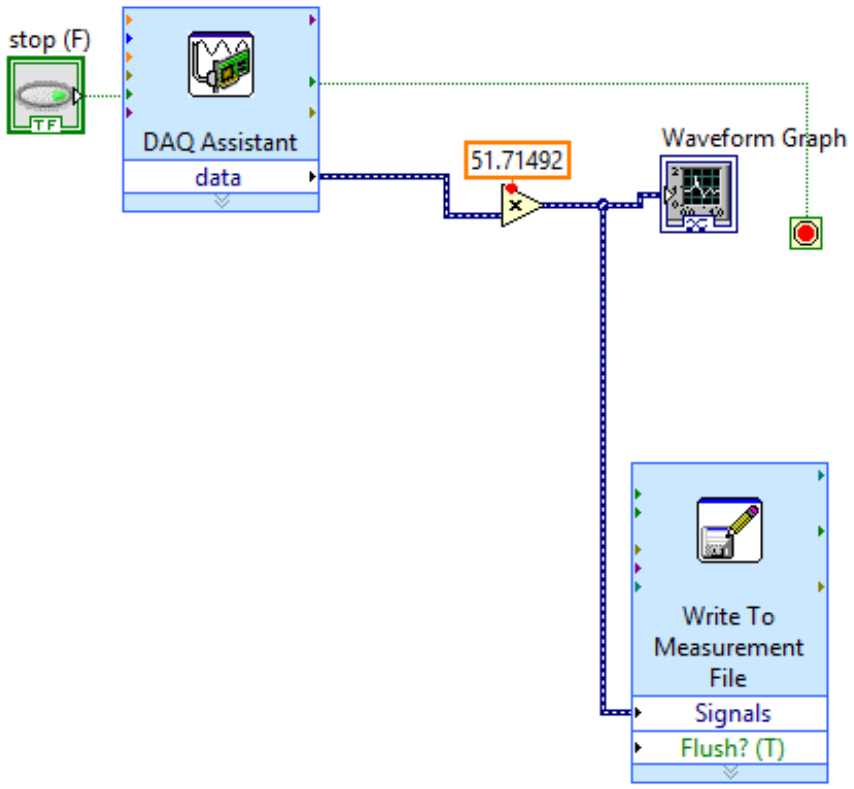

Figure 7: LabView VI used for the extraction of pressure data from the Deltran II pressure transducers. The y-axis of the waveform graph was multiplied by 51.71492 because the pressure transducers obtained pressure data in psi, and we were interested in mmHg. 1 psi = 51.71492 mmHg.

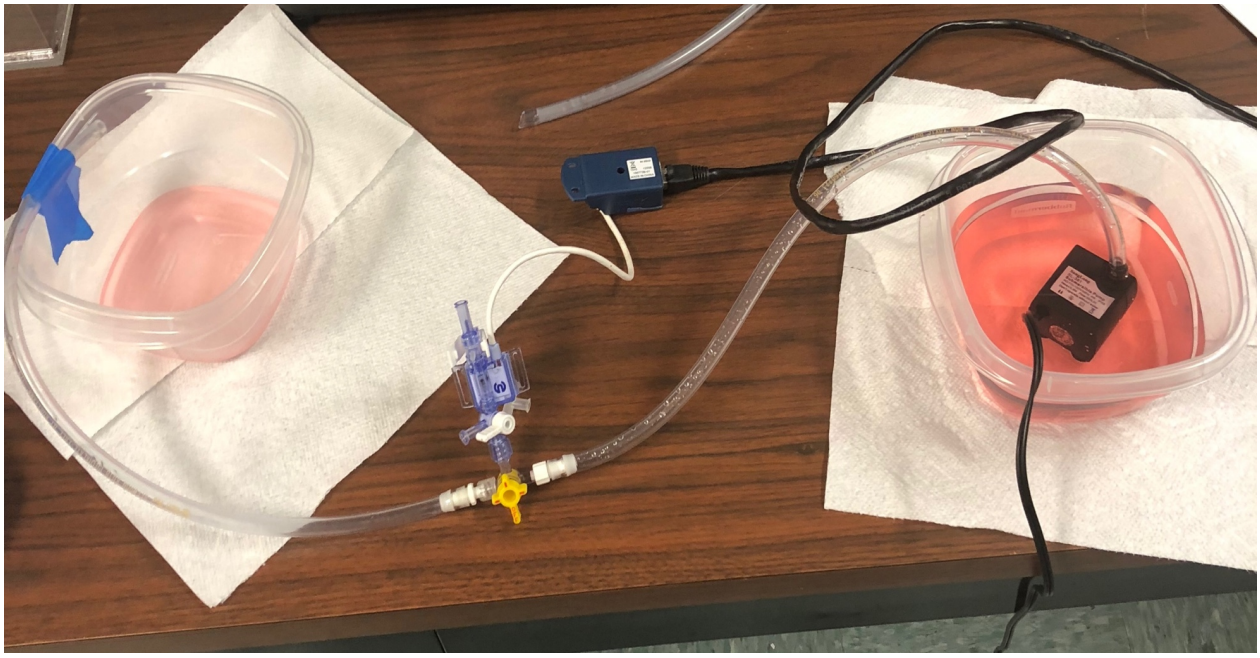

Figure 8: Mini flow loop setup for the verification of the functionality of the LabView block diagram.

Results & Analysis

Pulsatile Pump

Figure 9 shows the final pulsatile pump design and its specifications in a schematic created by the Cardiovascular Biomechanic's lab mechanical engineer, Sam Stephens. Sam came

up with the design and will be in charge of creating the pump. Currently, only a design for the pump exists.

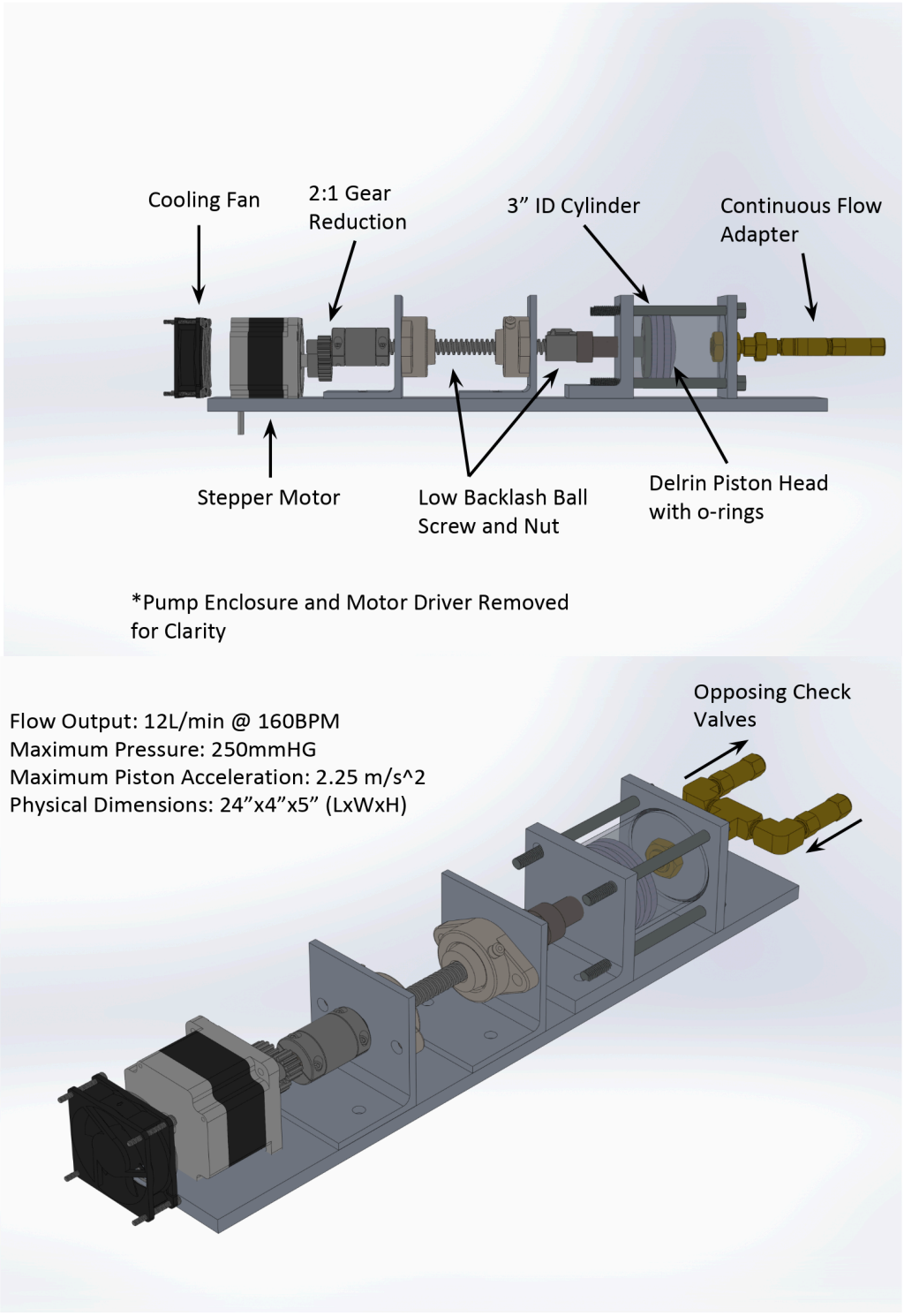

Figure 9: Design for the flow loop's pulsatile pump and its specifications.

Pressure Transducers

Figure 10 shows the data collected from the Deltran II pressure transducer when subject to pulsatile flow in the created mini flow loop. A continuous flow aquarium pump was used to supply water through the pressure transducer. Pulsatile flow was created by plugging and unplugging the pump so the flow of water would stop and start repeatedly. The measurements taken from LabView were exported into an Excel table and then converted to a graph in the same spreadsheet. LabView sampled pressure readings at a 25k Hz frequency. Although the created pulsatile flow was crude, it illustrated the pressure peaks created from such flow patterns. The peaks shown in this graph are analogous to the systolic pressure peaks that will be present in the pressure data taken from blood flow created by the pulsatile pump. It is important to recognize, though, that this pressure data was recorded from a single pressure transducer. When the in vitro flow loop is created, two pressure transducers will be taking pressure readings. One will be at the inlet, and one at the outlet of the stenosis. Thus, two pressure vs. time graphs will be needed to obtain a pressure gradient. To get two different graphs, another VI simply has to be created with the same code for the second transducer and run at the same time as the VI for the first transducer. These VI's will export pressure data to separate Excel files for analysis and extraction of pressure data. The pressure gradient will be obtained by acquiring the pressure values at the systolic peaks recorded by the transducer at the outlet of the stenosis, and subtracting these values from the pressures at the corresponding systolic peaks recorded by the transducer at the inlet of the stenosis. Time stamps are given for each pressure reading in the Excel table to confirm the readings and pressure peaks that correspond to each other.

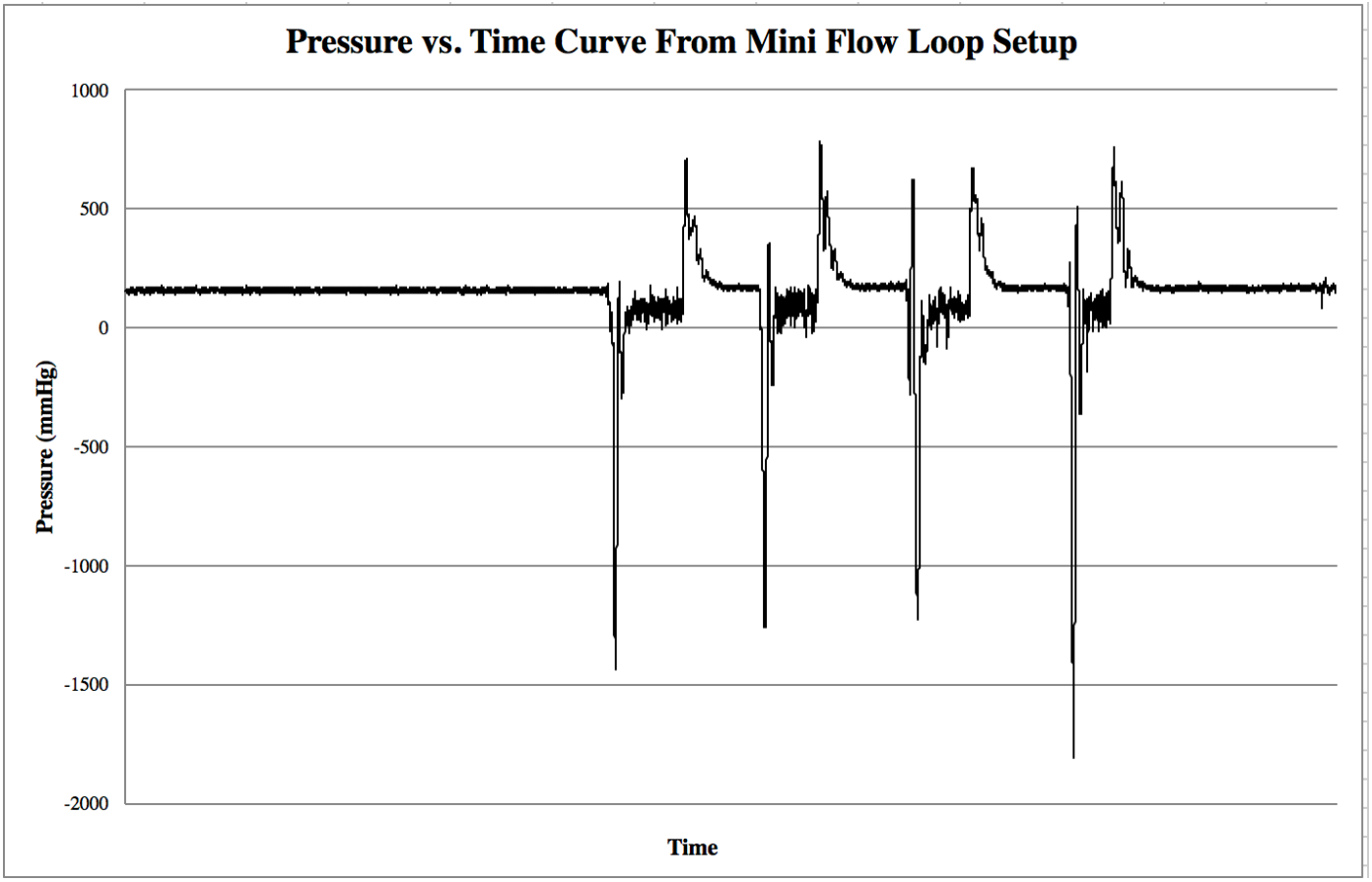

Figure 10: Pressure readings taken from single Deltran II pressure transducer during simulated pulsatile flow of water in mini flow loop setup.

Conclusion and Future Directions

The goal to complete the in vitro cardiac flow loop for validation of Vector Flow Imaging was left incomplete. The main components of the flow loop- the ballistics gel aortic arch phantom, the pressure transducers, and the pulsatile pump- were designed, and some created, for future incorporation into the flow loop. Silicone tubing that connects to each branch of the aortic arch phantom was also ordered. Future tasks and goals include creating the pulsatile pump, connecting the components of the in vitro cardiac flow loop together so that they are functioning properly, and running experiments and testing for comparisons of our obtained in vitro pressure gradients to that of VFI. A major part of connecting the flow loop is proper connection of the pressure transducers to the aortic arch phantom. Typically, pressure measurements of blood flow are taken in vivo by cardiac catheterization. This uses pressure transducers connected to the heart or vasculature via catheters. That is a possibility for this project. However, attempts at connecting the Deltran II pressure transducers to the vasculature without catheters will take place first. This may be done by creating holes at the inlet and outlet of the area of interest, and inserting the two transducers at either area so they are subject to the blood analog flow. In the future, it will be ideal to successfully isolate patient- specific stenotic aortas from MRI scans and printing them to create patient-specific aortic arch phantoms. The vasculature will then be more realistic and related to the application of diagnosing PAS. Until then, an area of stenosis can be created manually by narrowing a section of the healthy aortic arch phantom.

Although the in vitro flow loop was not able to be completed due to time constraints, the components' functionalities and design give strong reason to believe this in vitro flow loop will serve as a physiologically comparable way to validate the workings of VFI. By taking direct pressures from in vitro vasculature and using VFI ultrasound on the same vasculature as a

pulsatile flow of blood analog is pumped throughout, pressure gradients given in LabView and Excel can be compared to the pressure gradients derived from VFI images. The pressure gradient will be obtained from the pressure transducers by subtracting the peak systolic pressures measured at the outlet of the stenosis from that of the inlet of the stenosis. These peak systolic pressures can be found in the data exported from LabView into Excel as a table. The pressure gradient will be obtained from VFI by taking the peak blood flow velocities across the stenosis, and using that peak velocity in the simplified Bernoulli equation. Enough tests will be run that will either statistically support or refute the accuracy with which VFI can obtain these pressure gradients across the stenosis. Hopefully, conventional Doppler can be used to image the vasculature as well, to illustrate the superiority of VFI over conventional echocardiography in the diagnosis of pediatric aortic stenosis.

References:

1. Brown Brown JW, Ruzmetov M, Vijay P, Rodefeld MD, Turrentine MW. Surgery for aortic stenosis in children: a 40-year experience. The Annals of thoracic surgery. 2003 Nov 1;76(5):1398-411.
2. Saikrishnan N, Kumar G, Sawaya FJ, Lerakis S, Yoganathan AP. Accurate assessment of aortic stenosis: a review of diagnostic modalities and hemodynamics. Circulation. 2014 Jan 14;129(2):244-53.
3. Collins RT. Cardiovascular disease in Williams syndrome. Circulation. 2013 May 28;127(21):2125-34.
4. Kaplan P, Wang PP, Francke U. Williams (Williams Beuren) syndrome: a distinct neurobehavioral disorder. Journal of Child Neurology. 2001 Mar;16(3):177-90.
5. Gray JC, Krazinski AW, Schoepf UJ, Meinel FG, Pietris NP, Suranyi P, Hlavacek AM. Cardiovascular manifestations of Williams syndrome: imaging findings. Journal of cardiovascular computed tomography. 2013 Nov 1;7(6):400-7.
6. Champsaur G, Trusler GA, Mustard WT. Congenital discrete subvalvar aortic stenosis. Surgical experience and long-term follow-up in 20 paediatric patients. British heart journal. 1973 Apr;35(4):443.
7. Menges H, Brandenburg RO, Brown AL. The clinical, hemodynamic, and pathologic diagnosis of muscular subvalvular aortic stenosis. Circulation. 1961 Nov 1;24(5):1126-36.
8. Goldberg SJ, Allen HD, Sahn DJ. Pediatric and adolescent echocardiography: A handbook. Year Book Medical Publishers, Incorporated; 1980.
9. Hansen KL, Møller-Sørensen H, Pedersen MM, Hansen PM, Kjaergaard J, Lund JT, Nilsson JC, Jensen JA, Nielsen MB. First report on intraoperative vector flow imaging of the heart among patients with healthy and diseased aortic valves. Ultrasonics. 2015 Feb 1;56:243-50.
10. Udesen J, Jensen JA. Experimental investigation of transverse flow estimation using transverse oscillation. InUltrasonics, 2003 IEEE Symposium on 2003 Oct 5 (Vol. 2, pp. 1586-1589). IEEE.
11. Jensen JA. A new estimator for vector velocity estimation [medical ultrasonics]. IEEE transactions on ultrasonics, ferroelectrics, and frequency control. 2001 Jul;48(4):886-94.
12. Hansen KL. In-vivo studies of new vector velocity and adaptive spectral estimators in medical ultrasound. Danish medical bulletin. 2010 May;57(5):1-23.
13. Jensen JA. Estimation of blood velocities using ultrasound: a signal processing approach. Cambridge University Press; 1996 Mar 29.

14. Hansen KL, Møller-Sørensen H, Kjaergaard J, Jensen MB, Jensen JA, Nielsen MB. Aortic valve stenosis increases helical flow and flow complexity: a study of intra-operative cardiac vector flow imaging. Ultrasound in Medicine and Biology. 2017 Aug 1;43(8):1607-17.

15. Pasta S, Scardulla F, Rinaudo A, Raffa GM, D'Ancona G, Pilato M, Scardulla C. An in vitro phantom study on the role of the bird-beak configuration in endograft infolding in the aortic arch. Journal of Endovascular Therapy. 2016 Feb;23(1):172-81.

16. Altman, Philip L. Dittmer, Dorothy S.. (1972-1974). Biology Data Book, Volumes 1-3 (2nd Edition) - References. Federation of American Societies for Experimental Biology. Online version available at:

17. Sulaiman A, Roty C, Serfaty JM, Attia C, Huet L, Douek P. In vitro, nonrigid model of aortic arch aneurysm. Journal of Vascular and Interventional Radiology. 2008 Jun 1;19(6):919-24